Burrowing star-nosed moles (*Condylura cristata*) are not hypoxia-tolerant

DEVEREAUX[1], Maiah EM, CAMPBELL, Kevin L[2], MUNRO, Daniel[1], BLIER, Pierre U[3] and PAMENTER, Matthew E[1,4*]

[1]Department of Biology, University of Ottawa, Ottawa, ON, Canada

[2]Department of Biological Sciences, University of Manitoba, Winnipeg, Canada

[3]Départment de Biologie, L'Université du Québec à Rimouski, Rimouski, Canada

[4]University of Ottawa Brain and Mind Research Institute, Ottawa, ON, Canada

NSE TO ACUTE HYPOXIA

Keywords: respirometry, metabolism, plethysmography, hypoxic ventilatory response, fossorial, Talpidae

Abstract

Star-nosed moles (*Condylura cristata*) have an impressive diving performance and burrowing lifestyle, yet no ventilatory data are available for this or any other talpid mole species. We predicted that, like many other semi-aquatic and fossorial small mammals, star-nosed moles would (*i*) exhibit a blunted (*i.e.*, delayed or reduced) hypoxic ventilatory response, (*ii*) a reduced metabolic rate, and (*iii*) a lowered body temperature (T_b) in hypoxia. We thus non-invasively measured these variables from wild-caught star-nosed moles exposed to normoxia (21% O_2) or acute graded hypoxia (21-6% O_2). Surprisingly, star-nosed moles did not exhibit a blunted HVR

or decrease T_b in hypoxia, and only manifested a significant albeit small (<8%) depression of metabolic rate at 6% O_2 relative to normoxic controls. Unlike small rodents inhabiting similar niches, star-nosed moles are thus intolerant to hypoxia, which may reflect an evolutionary trade-off favouring the extreme sensory biology of this unusual insectivore

Introduction

While most adult mammals are largely intolerant of hypoxia, a few species inhabit niches in which they acutely or chronically experience low O_2 tensions (Boggs et al., 1984; Lacey EA, Patton JL, 2000; Roper et al., 2001; Shams et al., 2005). As environmental O_2 decreases, aerobic metabolism is curtailed and cells struggle to generate the required ATP for homeostasis (Buck and Pamenter, 2006; Hochachka, 1986). To compensate, animals that exploit hypoxic environments have evolved a range of physiological, molecular, and genetic adaptations (Dzal et al., 2015; Jiang et al., 2020). These specializations can be broadly categorized into mechanisms that decrease metabolic demand for O_2, and mechanisms that increase the delivery of O_2 to aerobic tissues.

Metabolic rate suppression, wherein the body's rate of O_2 consumption ($\dot{V}O_2$) decreases in concert with environmental O_2 availability, is an important strategy to mitigate the deleterious effects of hypoxia. The hypoxic metabolic response (HMR) may be comprised of various cellular and behavioural modifications; however, because the largest metabolic demand in small mammals is usually thermoregulation, downregulating the body temperature (T_b) setpoint and reducing core T_b are often major components of the HMR (Tattersall and Milsom, 2009). Indeed, concurrent declines in $\dot{V}O_2$ and T_b often occur in hypoxia-tolerant species (Frappell et al., 1992) and neonates (Teppema and Dahan, 2010) during hypoxic exposure. Comparatively, most terrestrial adult mammals are hypoxia-intolerant and exhibit little to no HMR or change in T_b in hypoxia (Frappell et al., 1992).

Whereas most hypoxia-adapted mammals rely primarily on reducing $\dot{V}O_2$ to tolerate low environmental O_2, most hypoxia-intolerant mammals instead increase O_2 supply. Central to this latter strategy is the hypoxic ventilatory response (HVR), a reflexive increase in breathing (Frappell et al., 1992; Iturriaga et al., 2016; Pamenter and Powell, 2016; Powell et al., 1998). In hypoxia-intolerant species, this response typically manifests at environmental O_2 levels as high as 18-15% (Arieli and Ar, 1979; Hemingway and Nahas, 1952). Comparatively, hypoxia-tolerant species exhibit a blunted HVR, and defer hyperventilating until environmental O_2 tensions drop below 5-10% (Barros et al., 2004; Boggs et al., 1998; Frappell et al., 1994; Ivy et al., 2020; Tomasco et al., 2010).

Star-nosed moles (*Condylura cristata*) are small (40-60g) non-hibernating fossorial mammals native to north-eastern North America, and are the only member of their subfamily (*Condylurinae*) within the family Talpidae (Hamilton, 1931; Petersen and Yates, 1980). They are distinguished by a mobile and highly mechanosensitive 22-tentacled snout that is used to search for invertebrate prey in both aquatic and subterranean settings (Catania and Kaas, 1996). Indeed, star-nosed moles are well adapted for underground life and dig extensive tunnel systems at depths of 3-60 cm in wet soils adjacent to wetlands and streams (Hickman, 1983; Rust, 1966). While gaseous measurements of star-nosed mole burrows are not available, soil moisture impedes gas exchange and exhibits an inverse relationship with O_2 tension within coast mole (*Scapanus orarius*) tunnels (Schaefer and Sadleir, 1979). As insectivores, the protein rich diet of *C. cristata* also contributes to a higher O_2 requirement for energy metabolism (Campbell et al., 2000; Pearson, 1947; Stephenson and Racey, 1995). Importantly, star-nosed moles are also competent thermoregulators and maintain a high and stable T_b of ~38°C, despite the challenge of living, and especially swimming, in sub-zero temperatures (Campbell et al., 1999; Campbell et al., 2000; McIntyre et al., 2002). This combination of lifestyle, diet, and high T_b presumably culminate in a substantially greater energetic demand than expected for their size, which is twice that of other fossorial mole species (Campbell et al., 1999).

In addition to living underground, star-nosed moles are accomplished divers (McIntyre et al., 2002). Advanced diving capabilities have been linked with hypoxia-tolerance due to relatively long periods spent without breathing (Meir et al., 2009; Willmore and Storey, 1997). Although these traits do not universally correlate to hypoxia tolerance, given their burrowing lifestyle and diving capabilities, we hypothesized that star-nosed moles would exhibit physiological adaptations to resist severe hypoxia, as occurs in other subterranean and diving mammals. We predicted this tolerance would be achieved in part through metabolic rate suppression, reduced thermogenesis, and a blunted HVR.

Methodology

Animals. Star-nosed moles (3 adults and 5 juveniles) of unknown sex were captured during June 2019 on private land in forested areas south of Saint-Anaclet-de-Lessard, Quebec, Canada, using Sherman and pitfall traps. Animals were housed at the Université du Québec à Rimouski (22°C, 20.95% O_2, 0.04% CO_2, 50% humidity) with ambient lighting synchronized to the external photoperiod. The moles were housed individually in modified, interconnected chambers. The first chamber (61×41×22 cm) was used exclusively for feeding (to permit food consumption monitoring and facilitate daily cleaning) and was connected by ABS pipe (1.5” diameter) to a nesting chamber (16×16×9 cm) filled with dried grass and located within a container (73×50×30 cm) furnished with ~10 cm of top-soil for the animals to freely burrow. Animals were fed 7-10 large nightcrawlers (~30-40 g) every 12 hrs. Twenty-four hrs after arriving at the animal facility, each mole was implanted with a RFID temperature transponder (Bio-Thermo, Destron Fearing, Langeskov, Denmark) unanesthetized via syringe along the back flank and given 48 hrs before experimentation to recover. The moles were not fasted prior to experimental trials and were allowed a minimum of one week between the normoxic and hypoxic experiments. Respective animal trials were performed at the same time of day to reduce confounding effects of individual circadian rhythms. All experimental procedures were approved by the University of Ottawa's Animal Care Committee (protocol #2535) in consultation with the Animal Care Committee from the Université du Québec à Rimouski, with animal trapping, husbandry, and experimentation conducted in accordance with the Animals for Research Act and the Canadian Council on Animal Care.

Whole-Body Plethysmography and Respirometry. A single, unrestrained mole was placed in a transparent 450 mL Plexiglas chamber connected in parallel to an identical (empty) reference chamber and closely monitored throughout each experimental trial. Experiments were performed at 22°C, to which animals were habituated prior to experimentation. The animal chamber was sealed and ventilated by positive pressure with gas mixtures set to the desired fractional gas composition by calibrated rotameters (Krohne, Duisburg, Germany). The flow rate of gas (FRi) was set to 400 mL/min, and was verified using a calibrated mass flow meter (M-Series, Alicat Scientific, Tuscon, AZ, USA). Humidity in the inspired/expired air was measured by passing the excurrent air through an RH-300 Water Vapour Pressure Analyzer (Sable Systems International, Las Vegas, NV, USA). The excurrent gas was then passed through desiccant media (Drierite, W.A. Hammond Drierite Co. Ltd., Xenia, OH, USA) before entering the CO_2 and O_2 analyzers (FC-10 O_2 and CA-10 CO_2 Analyzers, Sable Systems).

Animals were subjected to two different experimental protocols: 1) normoxia and 2) acute graded hypoxia. In the normoxia protocol, animals were exposed to 20.95% O_2/0.04% CO_2 for 3.5 hrs. In the hypoxia protocol, animals were first held in normoxia to establish a baseline, then four exposures of progressively deeper hypoxia, followed by a reoxygenation period (*i.e.*, 20.95, 15, 12, 9, 6, and then 20.95% O_2; balance N_2, 35 mins each). Animals were randomly assigned which protocol to receive first. The initial hypoxia protocol was to include a 3-5% O_2 step, but the mole in the first hypoxia trial suddenly and unexpectedly died once the chamber reached 5.2%, suggesting that O_2 tensions of <6% are below the lethal limit for the species. T_b was recorded non-invasively every 5 mins throughout all experiments using an RFID reader (Allflex USA Inc., Dallas, TX, USA) to scan the previously implanted RFID chips. The chamber temperature was recorded every 2 secs by a custom-built thermocouple.

Before each trial the O_2 and CO_2 analyzers were calibrated using 100% N_2 and compressed air (20.95% O_2, 0.04% CO_2, balance N_2). For the final 5 mins of each O_2 exposure, incurrent humidity and fractional O_2 (FiO_2) and CO_2 ($FiCO_2$) concentrations were measured by bypassing the experimental chamber and diverting air flow directly to the gas analyzers. Stable 30-sec measurements of incurrent gas concentrations and relative humidity (%) were then used as baselines for metabolic rate calculations (see below). In the hypoxia trials, incurrent gas concentrations were then changed to the desired O_2 level before returning airflow to the experimental chamber.

Animal ventilation causes pressure fluctuations due to changes in humidity and temperature between inspired and expired air that can be measured relative to a reference chamber to noninvasively monitor breathing (Jacky, 1978). We employed a differential pressure transducer (DP103-18, Validyne, Northridge, CA, USA) connected between the two chambers to amplify and continuously monitor this signal. Before each trial, the transducer was calibrated by injecting/withdrawing six known volumes of air (0.1, 0.2, 0.3, 0.4, 0.5, and 0.6 mL) ten times into the experimental chamber at a rate similar to the breathing rate of the test subjects.

Data Collection and Analysis. Because experiments were conducted in random order and not all star-nosed moles were tolerant to 6% O_2, sample size varied between the normoxic (*n* = 7) and hypoxic (*n* = 6-8) exposures. For the hypoxic dataset, two juvenile animals appeared to become distressed while in 6% O_2 and were immediately transferred to normoxia; hence only data to 9% O_2 were included for these individuals. Ventilatory and metabolic data were collected using LabChart software and analyzed in PowerLab (AD Instruments, Colorado Springs, CO, USA). Respiratory gas concentrations and pressure deflections were sampled at 1000 Hz. The 10-min interval between 20 and 30 mins of each gas exposure was analyzed to calculate mean excurrent fractional O_2 (FeO_2) and CO_2 ($FeCO_2$) concentrations and ventilatory parameters.

$\dot{V}O_2$ was calculated using equation 10.6 in Lighton (2008): $\dot{V}O_2$ ($mL{\bullet}min^{-1}{\bullet}Kg^{-1}$) = FRi [($FiO_2$ – $FeO_2$2) – FeO_2 ($FeCO_2$ – $FiCO_2$)]/(1 – FeO_2). The rate of CO_2 production ($\dot{V}CO_2$) was calculated using equation 10.7 from the same source: $\dot{V}CO_2$ ($mL{\bullet}min^{-1}{\bullet}Kg^{-1}$) = FRi [($FeCO_2$ – $FiCO_2$) – FeO_2 (FiO_2 – FeO_2)]/(1 – $FeCO_2$). The resulting $\dot{V}O_2$ and $\dot{V}CO_2$ values were divided by animal body mass for mass-specific comparisons. The respiratory exchange ratio (RER) was calculated as the ratio of $\dot{V}CO_2/\dot{V}O_2$. The % of O_2 extracted (eO_2) was calculated as: (FiO_2 – FeO_2)/FiO_2 × 100%.

To calculate tidal volume (V_T, mL•Kg^{-1}) and respiratory frequency (f_R, breath•min^{-1}) five breathing intervals were selected from within the same 10-minute period used for metabolic rate calculations, with each interval consisting of a minimum of 10 consecutive and clearly defined pressure oscillations, each of which was counted as one breath. The Drorbaugh and Fenn equation ($V_T = [P_m V_{cal} T_A(P_B-P_C)]/[P_{cal}(T_A(P_B-P_C)-T_C(P_B-P_A))]$) was used to calculate V_T (Drorbaugh and Fenn, 1955). P_m (measured in volts) is the pressure deflection corresponding to the expired breaths. The average cyclic maximum and minimum deflections were taken from each breathing interval. The difference represented the average total pressure deflection of a breath, P_m, while P_{cal} (volts) and V_{cal} (µl) are the pressure deflection and volume of a known calibrated volume, respectively. The average cyclic maximum and minimum deflection of each calibration set was plotted against the injected volume to create a linear relationship. The point on this line representing 0.2 mL was chosen as P_{cal} and V_{cal}. T_A and T_C are the animal body and chamber temperature (˚K), respectively, each recorded at the end of the 10-min period. P_B is the barometric pressure (mmHg) as measured by the O_2 analyzer. P_A (mmHg) is the vapour pressure of water at the animal's $T_{A,}$ and P_C is the partial pressure of water vapour (mmHg) in the incurrent gas stream. P_A was calculated using the relative humidity (%) of excurrent air, T_b (˚C), and barometric pressure (mmHg). P_C was determined from relative humidity (%) of incurrent air, chamber temperature (˚C), and barometric pressure (mmHg). Minute ventilation ($\dot{V}_E$, mL•min^{-1}•Kg^{-1}) was calculated as the product of f_R and V_T. The air convection requirement of O_2 and CO_2 ($ACRO_2$ and $ACRCO_2$, respectively) were calculated as the quotient of $\dot{V}_E$ and $\dot{V}O_2$ or $\dot{V}CO_2$, respectively.

Statistical analysis. Statistical analysis was performed using commercial software (Prism v. 8.4.2, GraphPad Software Inc., CA, USA). All values are presented as mean ± 1 S.E.M, where $p < 0.05$ was the threshold for significance. Due to the wide variance, sphericity was not assumed but was corrected for using a Geisser-Greenhouse correction. Statistical significance was evaluated using a mixed-effects model analysis (REML) to test for interactions between two independent variables: normoxia and O_2 level (20.95, 15, 12, 9, 6, and 20.95% O_2). Tukey's and Sidak's multiple comparisons tests were performed on each dependent variable to determine significance. Respirometry and ventilatory data were qualitatively similar whether mass-corrected or not mass-corrected, and so data are presented normalized to body mass, where appropriate. Adult and juvenile data was pooled as no differences were found across O_2 conditions/time points for any of the evaluated parameters (supplementary Table 1).

Results and Discussion

Star-nosed moles have a high lethal threshold to hypoxia. Star-nosed moles possess large spade-like forepaws and, like fossorial rodents, are morphologically specialized to exploit the subterranean niche. It is thus somewhat surprising that, despite their long evolutionary history of fossoriality (Petersen and Yates, 1980), the lethal hypoxic threshold for this species appears to be near 6% O_2, which is comparable to mice and humans (Milroy, 2018; Zhang et al., 2004). By contrast, the lethal hypoxic threshold of fossorial and subterranean rodents typically spans 0-3% O_2 (Ivy et al., 2020; Park et al., 2017).

Star-nosed moles have a weak HMR and do not alter thermogenesis in acute hypoxia. We found no pronounced metabolic or thermoregulatory responses to hypoxia in this species (supplementary Tables 2, 3). Specifically, $\dot{V}O_2$ was not strongly affected by hypoxia, decreasing only in 6% O_2 (by 7.4% relative to normoxia; $p = 0.0308$, $F_{5,62} = 3.855$, Fig. 1A). By contrast, $\dot{V}CO_2$ was unchanged ($p = 0.4468$, $F_{5,62} = 1.438$, Fig. 1B). This finding is consistent with a recent genome-wide analysis of five subterranean species, which suggested that numerous positively selected genes of star-nosed moles are linked to the maintenance of a high energy supply (Jiang et al., 2020).

A minimal HMR is commonly observed in hypoxia-intolerant and non-fossorial small mammals (Frappell et al., 1992). Conversely, hypoxia-tolerant mammals manifest a more robust HMR that ranges from a 48-85% reduction in $\dot{V}O_2$ (Frappell et al., 1992; Guppy and Withers, 1999; Ivy et al., 2020), and is typically initiated at much higher O_2 tensions (~18-10% O_2) than hypoxia-intolerant species (Devereaux and Pamenter, 2020; Ivy et al., 2020; Walsh et al., 1996). By contrast, the $\dot{V}O_2$ of star-nosed moles was only significantly below normoxia controls at 6% O_2, but was not significantly lower than observed during other hypoxia steps (Fig. 1A).

Thermogenesis is an energetically expensive process, particularly in small mammals (Ballesteros et al., 2018); thus, reducing thermogenesis is a common strategy of metabolic rate suppression in hypoxia-tolerant species. Consistent with results from hypoxia-intolerant species (Frappell et al., 1992), we did not observe a drop in T_b in hypoxia ($p > 0.999$, $F_{5,62} = 0.6243$, Fig. 1D). Conversely, strategies to markedly lower T_b and reduce overall O_2 consumption have been observed in many hypoxia-tolerant species (Houlahan et al., 2018; Ilacqua et al., 2017; Mortola and Feher, 1998; Nilsson and Renshaw, 2004; Wood and Gonzales, 1996).

Although there was little to no change in both metabolic rate and T_b with hypoxia, the RER increased from ~0.8 in normoxia trials to ~1.0 in all hypoxia exposures, but only reached significance at 6% O_2 (p = 0.0011, $F_{5,62}$ = 15.09, Fig. 1C). This shift is indicative of a metabolic fuel switch from lipids/proteins to carbohydrates. Such a shift is consistent with an upregulation of anaerobic carbohydrate breakdown during acute hypoxia to sustain cellular function. Increased reliance on anaerobic pathways typically results in the accumulation of acidic end products in metabolically active tissues, the clearance of which requires O_2 (Coffman, 1963; Lewis et al., 2007; Maxime et al., 2000; Plambech et al., 2013; Svendsen et al., 2012). Indeed, the observed shift in RER was rapidly reversed following reoxygenation via a sharp increase in $\dot{V}O_2$ (Fig. 1A), which is consistent with the accumulation of an O_2 debt in hypoxia. Adaptive mechanisms that prevent the formation of an O_2 debt, such as use of alternate energy pathways or enhanced pH buffering, are common in hypoxia-tolerant species (Jackson et al., 1996; Park et al., 2017).

Since star-nosed moles were not fasted prior to experimentation and have a protein-rich insectivorous diet (Campbell et al., 2000), it is also possible that the observed metabolic fuel switch to primarily carbohydrates in hypoxia may have resulted in the accumulation of protein-based substrates. Increased $\dot{V}O_2$ upon reoxygenation may indicate a return to protein-based metabolism, which is more O_2 intensive. Importantly, this possibility accounts for the simultaneously elevated $\dot{V}O_2$ and normoxic-level RER (~0.7) following hypoxia, whereas an O_2 debt would more likely coincide with an RER below normoxic levels (Kaminsky et al., 1990; Takala, 1997).

Star-nosed moles do not have a blunted HVR. Most adult mammals increase ventilation in hypoxia (Frappell et al., 1992; Powell et al., 1998); however, the hypoxic threshold at which this response is initiated tends to be strongly blunted in hypoxia-tolerant species (Devereaux and Pamenter, 2020; Ivy et al., 2020; Tomasco et al., 2010). By contrast, star-nosed moles exhibited a robust HVR that was not blunted, in that both f_R and $ACRO_2$ were significantly increased in 15% O_2. This activation threshold is inconsistent with observations from other subterranean and hypoxia-tolerant species. Instead, it is similar to that of non-fossorial species such as dogs, rats, and rabbits (HVR initiated at 15-16% O_2 (Cao et al., 1992; Holloway and Heath, 1984; Sokołowska and Pokorski, 2006)). Notably, both these variables continued to increase with progressively deeper hypoxia, with f_R increasing by 167% in 6% O_2 ($p < 0.0001$, $F_{5,62} = 53.15$, Fig. 2B) and $ACRO_2$ increasing by 341% at this same gas tension ($p < 0.0001$, $F_{5,62} = 41.13$, Fig. 2D).

In addition to f_R, V_T also increased in acute hypoxia, reaching significance in 12% O_2 and peaking at 53% over baseline in 6% O_2 ($p = 0.0048$, $F_{5,62} = 6.948$, Fig. 2C). Accordingly, $\dot{V}_E$ was also elevated in 12% O_2 and progressively increased to a maximum of 320% above baseline in 6% O_2 ($p < 0.0001$, $F_{5,62} = 51.57$, Fig. 2A). $ACRCO_2$ increased by 247% over this same interval ($p < 0.0001$, $F_{5,62} = 25.62$, Fig. 2E). Of the total increase in $\dot{V}_E$ at 6% O_2 (the most severe level of hypoxia tolerated), 63.5% was attributable to the increase in f_R and 36.5% to the increase in V_T. Although breathing more deeply requires greater energy expenditure, increasing V_T increases non-dead space ventilation, thereby maximizing the gas-exchange of each breath (Tenney and Boggs, 2011; Vitalis and Milsom, 1986). Relying predominantly on f_R to increase O_2 supply, as observed here, is a less efficient strategy as it results in a high degree of dead-space ventilation. The HVR of non-hypoxia-tolerant species are predominately mediated by increases in f_R

(Izumizaki et al., 2004; Morris and Gozal, 2004), whereas hypoxia-adapted species tend to increase V_T (Boggs et al., 1984; Devereaux and Pamenter, 2020).

Interestingly, eO_2 was also significantly elevated by 12% O_2 and reached a maximum 240% increase in 6% O_2 ($p < 0.0001$, $F_{5,62} = 69.54$, Fig. 2F). eO_2 is the fraction of inhaled O_2 that is absorbed into the body and is an indirect indicator of mechanisms that promote O_2 supply during hypoxia, such as increases in blood-O_2 affinity (Ar et al., 1977; Johansen et al., 1976), gas diffusion, hematocrit, and/or cardiac output. The nearly 3.5-fold increase in eO_2 suggests that compensatory mechanisms are robustly activated in star-nosed moles during hypoxia. While the blood O_2 affinity of *C. cristata* (22.5 mmHg at 36°C) is generally slightly lower than that of fully fossorial moles (Campbell et al., 2010; Quilliam et al., 1971), it is markedly higher than similarly sized non-subterranean mammals. Consistent with genome analysis revealing an enrichment of genes for respiratory gas exchange (Jiang et al., 2020), star-nosed moles also exhibit an enlarged lung volume, high blood hematocrit (~50%) and blood carrying capacity, and elevated muscle myoglobin content relative to fossorial moles (McIntyre et al., 2002). These traits align with the observed increase in eO_2 and presumably are important for extending dive durations of this species. Finally, and unlike non-talpid subterranean lineages, star-nosed moles do not have expanded families of hypoxia-related genes relative to non-subterranean species (Jiang et al., 2020), supporting our finding that their metabolic and ventilatory responses are more in line with those of hypoxia-intolerant species.

Conclusions. Our results refute our *a priori* prediction that star-nosed moles are strongly hypoxia-tolerant. Specifically, their relatively high lethal hypoxic (6% O_2) and HVR thresholds (12-15% O_2), the minimal HMR, and lack of T_b reduction in hypoxia are more similar to the phenotype of hypoxia-intolerant and non-fossorial mammals, and starkly contrast with the physiological responses of hypoxia-tolerant rodents.

Whereas metabolic depression and reduced thermogenesis are often key contributors to hypoxia-tolerance, such responses may be maladaptive for star-nosed moles due to their unusual biology and feeding behaviour. For example, the distribution of star-nosed moles is substantially further north than other North American talpids, which, coupled with their semi-aquatic habits and an inability to exploit facultative torpor, has presumably selected for a high metabolic intensity and stable T_b (Campbell et al., 1999). Indeed, consistent with results of previous studies (Campbell et al., 2000), our captive moles consumed more than their body mass per day.

Unlike hypoxia-tolerant rodents, star-nosed moles are voracious predators and meet their high energy requirements by actively searching both their invertebrate-dense tunnel systems and adjacent underwater areas (Hamilton, 1931). Further, the elaborate star-nosed mole nose has undergone strong directional selection for speed—capable of >10 prey searches per second—allowing them to consume hundreds of prey per minute (Catania and Remple, 2005). The likely consequence of their 'hard-wired' high metabolic intensity lifestyle and extreme sensory motor specialization for speed is a high continual supply of oxygen. Thus, despite exploiting shallow burrow systems constructed in mucky soils with limited gas exchange, star-nosed moles exhibit a relative hypoxia-intolerant phenotype, which is presumably mitigated by behavioural and respiratory adaptations for semi-aquatic life that maximize oxygen uptake and delivery (McIntyre et al., 2002). Whether or not a similar phenotype is shared by other fossorial talpid moles, which tend to exhibit lower metabolic intensities, more labile T_b's, and less specialized nasal somatosensory systems, is unknown and worthy of further investigation.

References

Ar, A., Arieli, R. and Shkolnik, A. (1977). Blood-gas properties and function in the fossorial mole rat under normal and hypoxic-hypercapnic atmospheric conditions. *Respir. Physiol.* **30**, 201–218.

Arieli, R. and Ar, A. (1979). Ventilation of a fossorial mammal (*Spalax ehrenbergi*) in hypoxic and hypercapnic conditions. *J. Appl. Physiol. Respir. Environ. Exerc. Physiol.* **47**, 1011–1017.

Ballesteros, F. J., Martinez, V. J., Luque, B., Lacasa, L., Valor, E. and Moya, A. (2018). On the thermodynamic origin of metabolic scaling. *Sci. Rep.* **8**, 1–10.

Barros, R. C. H., Abe, A. S., Cárnio, E. C. and Branco, L. G. S. (2004). Regulation of breathing and body temperature of a burrowing rodent during hypoxic-hypercapnia. *Comp. Biochem. Physiol. A Mol. Integr. Physiol.* **138**, 97–104.

Boggs, D. F., Kilgore, D. L. and Birchard, G. F. (1984). Respiratory physiology of burrowing mammals and birds. *Comp. Biochem. Physiol. A Mol. Integr. Physiol.* **77**, 1–7.

Boggs, D. F., Frappell, P. B. and Kilgore, D. L. (1998). Ventilatory, cardiovascular and metabolic responses to hypoxia and hypercapnia in the armadillo. *Respir. Physiol.* **113**, 101–109.

Buck, L. T. and Pamenter, M. E. (2006). Adaptive responses of vertebrate neurons to anoxia - Matching supply to demand. *Respir. Physiol. Neurobiol.* **154**, 226–240.

Campbell, K. L., McIntyre, I. W. and MacArthur, R. A. (1999). Fasting metabolism and thermoregulatory competence of the star-nosed mole, *Condylura cristata* (Talpidae: Condylurinae). *Comp. Biochem. Physiol. A Mol. Integr. Physiol.* **123**, 293–298.

Campbell, K. L., McIntyre, I. W. and MacArthur, R. A. (2000). Postprandial heat increment does not substitute for active thermogenesis in cold-challenged star-nosed moles. *J. Exp. Biol.*. **203**, 301–310.

Campbell, K. L., Storz, J. F., Signore, A. V., Moriyama, H., Catania, K. C., Payson, A. P., Bonaventura, J., Stetefeld, J. and Weber, R. E. (2010). Molecular basis of a novel adaptation to hypoxic-hypercapnia in a strictly fossorial mole. *BMC Evol. Biol.* **10**, 214.

Cao, K. Y., Zwillich, C. W., Berthon-Jones, M. and Sullivan, C. E. (1992). Increased normoxic ventilation induced by repetitive hypoxia in conscious dogs. *J. Appl. Physiol.* **73**, 2083–2088.

Catania, K. C. (2006). Underwater “sniffing” by semi-aquatic mammals. *Nature* **444**, 1024–1025.

Catania, K. C. and Kaas, J. H. (1996). The unusual nose and brain of the star-nosed mole: A star in the brain. *Bioscience* **46**, 578–586.

Catania, K. C. and Remple, F. E. (2005). Asymptotic prey profitability drives star-nosed moles to the foraging speed limit. *Nature* **433**, 519–522.

Coffman, J. D. (1963). Blood flow and oxygen debt repayment in exercising skeletal muscle. *Am. J. Physiol.* **205**, 365–369.

Devereaux, M. E. M. and Pamenter, M. E. (2020). Fossorial giant Zambian mole-rats have blunted ventilatory responses to environmental hypoxia and hypercapnia. *Comp. Biochem. Physiol. A Mol. Integr. Physiol.* **243**, 110672.

Drorbaugh, J. E. and Fenn, W. O. (1955). A barometric method for measuring ventilation in newborn infants. *Pediatrics* **16**, 81–87.

Dzal, Y. A., Jenkin, S. E. M., Lague, S. L., Reichert, M. N., York, J. M. and Pamenter, M. E. (2015). Oxygen in demand: How oxygen has shaped vertebrate physiology. *Comp. Biochem. Physiol. A Mol. Integr. Physiol.* **186**, 4–26.

Frappell, P., Lanthier, C., Baudinette, R. V and Mortola, J. P. (1992). Metabolism and ventilation in acute hypoxia: A comparative analysis in small mammalian species. *Am. J. Physiol. - Regul. Integr. Comp. Physiol.* **262**, R1040-R1046.

Frappell, P. B., Franklin, C. E. and Grigg, G. C. (1994). Ventilatory and metabolic responses to hypoxia in the echidna, Tachyglossus aculeatus. *Am. J. Physiol. - Regul. Integr. Comp. Physiol.* **267**, R1510–R1515.

Guppy, M. and Withers, P. (1999). Metabolic depression in animals: physiological perspectives and biochemical generalizations. *Biol. Rev. Camb. Philos. Soc.* **74**, 1–40.

Hamilton, W. J. (1931). Habits of the star-nosed mole, *Condylura cristata*. *J. Mammal.* **12**, 345.

Hemingway, A. and Nahas, G. G. (1952). Effect of hypoxia on the metabolic response to cold. *J. Appl. Physiol.* **5**, 267–272.

Herbert, N. A. and Steffensen, J. F. (2005). The response of Atlantic cod, Gadus morhua, to progressive hypoxia: Fish swimming speed and physiological stress. *Mar. Biol.* **147**, 1403–1412.

Hickman, G. C. (1983). Influence of the semiaquatic habit in determining burrow structure of the star-nosed mole (*Condylura cristata*). *Can. J. Zool.* **61**, 1688–1692.

Hochachka, P. W. (1986). Defense strategies against hypoxia and hypothermia. *Science.* **231**, 234–241.

Holloway, D. A. and Heath, A. G. (1984). Ventilatory changes in the golden hamster, *Mesocricetus auratus*, compared with the laboratory rat, *Rattus norvegicus*, during hypercapnia and/or hypoxia. *Comp. Biochem. Physiol. A Mol. Integr. Physiol.* **77**, 267–273.

Houlahan, C. R., Kirby, A. M., Dzal, Y. A., Fairman, G. D. and Pamenter, M. E. (2018). Divergent behavioural responses to acute hypoxia between individuals and groups of naked mole rats. *Comp. Biochem. Physiol. B Biochem.Mol. Biol.* **224**, 38–44.

Ilacqua, A. N., Kirby, A. M. and Pamenter, M. E. (2017). Behavioural responses of naked mole rats to acute hypoxia and anoxia. *Biol. Lett.* **13**, 20170545.

Iturriaga, R., Del Rio, R., Idiaquez, J. and Somers, V. K. (2016). Carotid body chemoreceptors, sympathetic neural activation, and cardiometabolic disease. *Biol. Res.* **49**, 1–9.

Ivy, C. M., Sprenger, R. J., Bennett, N. C., Jaarsveld, B., Hart, D. W., Kirby, A. M., Yaghoubi, D., Storey, K. B., Milsom, W. K. and Pamenter, M. E. (2020). The hypoxia tolerance of eight related African mole- rat species rivals that of naked mole- rats, despite divergent ventilatory and metabolic strategies in severe hypoxia. *Acta Physiol.* **228**, e13436.

Izumizaki, M., Pokorski, M. and Homma, I. (2004). Role of the carotid bodies in chemosensory ventilatory responses in the anesthetized mouse. *J. Appl. Physiol.* **97**, 1401–1407.

Jackson, D. C., Toney, V. I. and Okamoto, S. (1996). Lactate distribution and metabolism during and after anoxia in the turtle, *Chrysemys picta bellii*. *Am. J. Physiol.* **271**, R409-R416.

Jacky, J. P. (1978). A plethysmograph for long-term measurements of ventilation in unrestrained animals. *J. Appl. Physiol. Respir. Environ. Exerc. Physiol.* **45**, 644–647.

Jiang, M., Shi, L., Li, X., Dong, Q., Sun, H., Du, Y., Zhang, Y., Shao, T., Cheng, H., Chen, W., et al. (2020). Genome- wide adaptive evolution to underground stresses in subterranean mammals: Hypoxia adaption, immunity promotion, and sensory specialization. *Ecol. Evol.* **10**, 7377–7388.

Johansen, K., Lykkeboe, G., Weber, R. E. and Maloiy, G. M. O. (1976). Blood respiratory properties in the naked mole rat *Heterocephalus glaber*, a mammal of low body temperature. *Respir. Physiol.* **28**, 303–314.

Kaminsky, L. A., Padjen, S. and LaHam-Saeger, J. (1990). Effect of split exercise sessions on excess post-exercise oxygen consumption. *Br. J. Sports Med.* **24**, 95–98.

Lacey EA, Patton JL, C. G. (2000). Life Underground: The biology of subterranean rodents. *Univ. Chicago Press* 84.

Lefrançois, C., Ferrari, R. S., Moreira Da Silva, J. and Domenici, P. (2009). The effect of progressive hypoxia on spontaneous activity in single and shoaling golden grey mullet *Liza aurata*. *J. Fish Biol.* **75**, 1615–1625.

Lewis, J. M., Costa, I., Val, A. L., Almeida-Val, V. M. F., Gamperl, A. K. and Driedzic, W. R. (2007). Responses to hypoxia and recovery: Repayment of oxygen debt is not associated with compensatory protein synthesis in the Amazonian cichlid, *Astronotus ocellatus*. *J. Exp. Biol.* **210**, 1935–1943.

Lighton, J. R. B. (2008). *Measuring Metabolic Rates: A Manual for Scientists*. Oxford University Press.

Livanova, L. M., Luk'ianova, L. D. and Torshin, V. I. (1993). [The effect of long-term adaptation to hypoxia on the open-field behavioral reactions in rats with different types of behavior]. *Zh. Vyssh. Nerv. Deiat. Im. I P Pavlova* **43**, 808–817.

Maxime, V., Pichavant, K., Boeuf, G. and Nonnotte, G. (2000). Effects of hypoxia on respiratory physiology of turbot, *Scophthalmus maximus*. *Fish Physiol. Biochem.* **22**, 51–59.

McIntyre, I. W., Campbell, K. L. and MacArthur, R. A. (2002). Body oxygen stores, aerobic dive limits and diving behaviour of the star-nosed mole (*Condylura cristata*) and comparisons with non-aquatic talpids. *J. Exp. Biol.* **205**, 45–54.

Meir, J. U., Champagne, C. D., Costa, D. P., Williams, C. L. and Ponganis, P. J. (2009). Extreme hypoxemic tolerance and blood oxygen depletion in diving elephant seals. *Am. J. Physiol. - Regul. Integr. Comp. Physiol.* **297**, 927–939.

Milroy, C. M. (2018). Deaths from environmental hypoxia and raised carbon dioxide. *Acad. Forensic Pathol.* **8**, 2–7.

Morris, K. F. and Gozal, D. (2004). Persistent respiratory changes following intermittent hypoxic stimulation in cats and human beings. *Respir. Physiol. Neurobiol.* **140**, 1–8.

Mortola, J. P. and Feher, C. (1998). Hypoxia inhibits cold-induced huddling in rat pups. *Respir. Physiol.* **113**, 213–222.

Nilsson, G. E. and Renshaw, G. M. C. (2004). Hypoxic survival strategies in two fishes: Extreme anoxia tolerance in the North European crucian carp and natural hypoxic preconditioning in a coral-reef shark. *J. Exp. Biol.* **207**, 3131–3139.

Pamenter, M. E. and Powell, F. L. (2016). Time domains of the hypoxic ventilatory response and their molecular basis. *Compr. Physiol.* **6**, 1345–1385.

Park, T. J., Reznick, J., Peterson, B. L., Blass, G., Omerbašić, D., Bennett, N. C., Kuich, P. H. J. L., Zasada, C., Browe, B. M., Hamann, W., et al. (2017). Fructose-driven glycolysis supports anoxia resistance in the naked mole-rat. *Science.* **356**, 307–311.

Pearson, O. P. (1947). The rate of metabolism of some small mammals. *Ecology* **28**, 127–145.

Petersen, K. E. and Yates, T. L. (1980). *Condylura cristata*. *Mamm. Species* **129**, 1–4.

Plambech, M., Van Deurs, M., Steffensen, J. F., Tirsgaard, B. and Behrens, J. W. (2013). Excess post-hypoxic oxygen consumption in Atlantic cod *Gadus morhua*. *J. Fish Biol.* **83**, 396–403.

Powell, F. L., Milsom, W. K. and Mitchell, G. S. (1998). Time domains of the hypoxic ventilatory response. *Respir. Physiol.* **112**, 123–134.

Quilliam, T. A., Clarke, J. A. and Salsbury, A. J. (1971). The ecological significance of certain new haematological findings in the mole and hedgehog. *Comp. Biochem. Physiol. A Mol. Integr. Physiol.* **40**, 89–102.

Roper, T. J., Bennett, N. C., Conradt, L. and Molteno, A. J. (2001). Environmental conditions in burrows of two species of African mole-rat, *Georhychus capensis* and *Cryptomys damarensis*. *J. Zool.* **254**, 101–107.

Rust, C. C. (1966). Notes on the star-nosed mole (*Condylura cristata*). *J. Mammal.* **47**, 538.

Schaefer, V. H. and Sadleir, R. M. F. S. (1979). Concentrations of carbon dioxide and oxygen in mole tunnels. *Acta Theriol. (Warsz).* **24**, 267–271.

Shams, I., Avivi, A. and Nevo, E. (2005). Oxygen and carbon dioxide fluctuations in burrows of subterranean blind mole rats indicate tolerance to hypoxic-hypercapnic stresses. *Comp. Biochem. Physiol. A Mol. Integr. Physiol.* **142**, 376–382.

Sokołowska, B. and Pokorski, M. (2006). Ventilatory augmentation by acute intermittent hypoxia in the rabbit. *J. Physiol. Pharmacol.* **57 Suppl 4**, 341–347.

Stephenson, P. J. and Racey, P. A. (1995). Resting metabolic rate and reproduction in the Insectivora. *Comp. Biochem. Physiol. A Mol. Integr. Physiol.* **112**, 215–223.

Svendsen, J. C., Steffensen, J. F., Aarestrup, K., Frisk, M., Etzerodt, A. and Jyde, M. (2012). Excess posthypoxic oxygen consumption in rainbow trout (*Oncorhynchus mykiss*): Recovery in normoxia and hypoxia. *Can. J. Zool.* **90**, 1–11.

Takala, J. (1997). Oxygen consumption and carbon dioxide production: Physiological basis and practical application in intensive care. IN *Anaesthesia, Pain, Intensive Care Emerg. Med. — A.P.I.C.E.* 155–162.

Tattersall, G. J. and Milsom, W. K. (2009). Hypoxia reduces the hypothalamic thermogenic threshold and thermosensitivity. *J. Physiol.* **587**, 5259–5274.

Tenney, S. M. and Boggs, D. F. (2011). Comparative mammalian respiratory control. *Compr. Physiol.* 833-855.

Teppema, L. J. and Dahan, A. (2010). The ventilatory response to hypoxia in mammals: Mechanisms, measurement, and analysis. *Physiol. Rev.* **90**, 675–754.

Tomasco, I. H., del Río, R., Iturriaga, R. and Bozinovic, F. (2010). Comparative respiratory strategies of subterranean and fossorial octodontid rodents to cope with hypoxic and hypercapnic atmospheres. *J. Comp. Physiol. B Biochem. Syst. Environ. Physiol.* **180**, 877–884.

Vitalis, B. Y. T. Z. and Milsom, W. K. (1986). Mechanical analysis of spontaneous breathing in the semi-aquatic turtle, *Pseudemys scripta*. *J. Exp. Biol.* **125**, 137–155.

Walsh, J. P., Boggs, D. F. and Kilgore, D. L. (1996). Ventilatory and metabolic responses of a bat, *Phyllostomus discolor*, to hypoxia and CO_2: implications for the allometry of respiratory control. *J. Comp. Physiol. B Biochem. Syst. Environ. Physiol.* **166**, 351–358.

Willmore, W. G. and Storey, K. B. (1997). Antioxidant systems and anoxia tolerance in a freshwater turtle *Trachemys scripta elegans*. *Mol. Cell. Biochem.* **170**, 177–185.

Wood, S. C. and Gonzales, R. (1996). Hypothermia in hypoxic animals: Mechanisms, mediators, and functional significance. *Comp. Biochem. Physiol. B Biochem. Mol. Biol.* **113**, 37–43.

Zhang, S. X. L., Miller, J. J., Gozal, D. and Wang, Y. (2004). Whole-body hypoxic preconditioning protects mice against acute hypoxia by improving lung function. *J. Appl. Physiol.* **96**, 392–397.

Figures

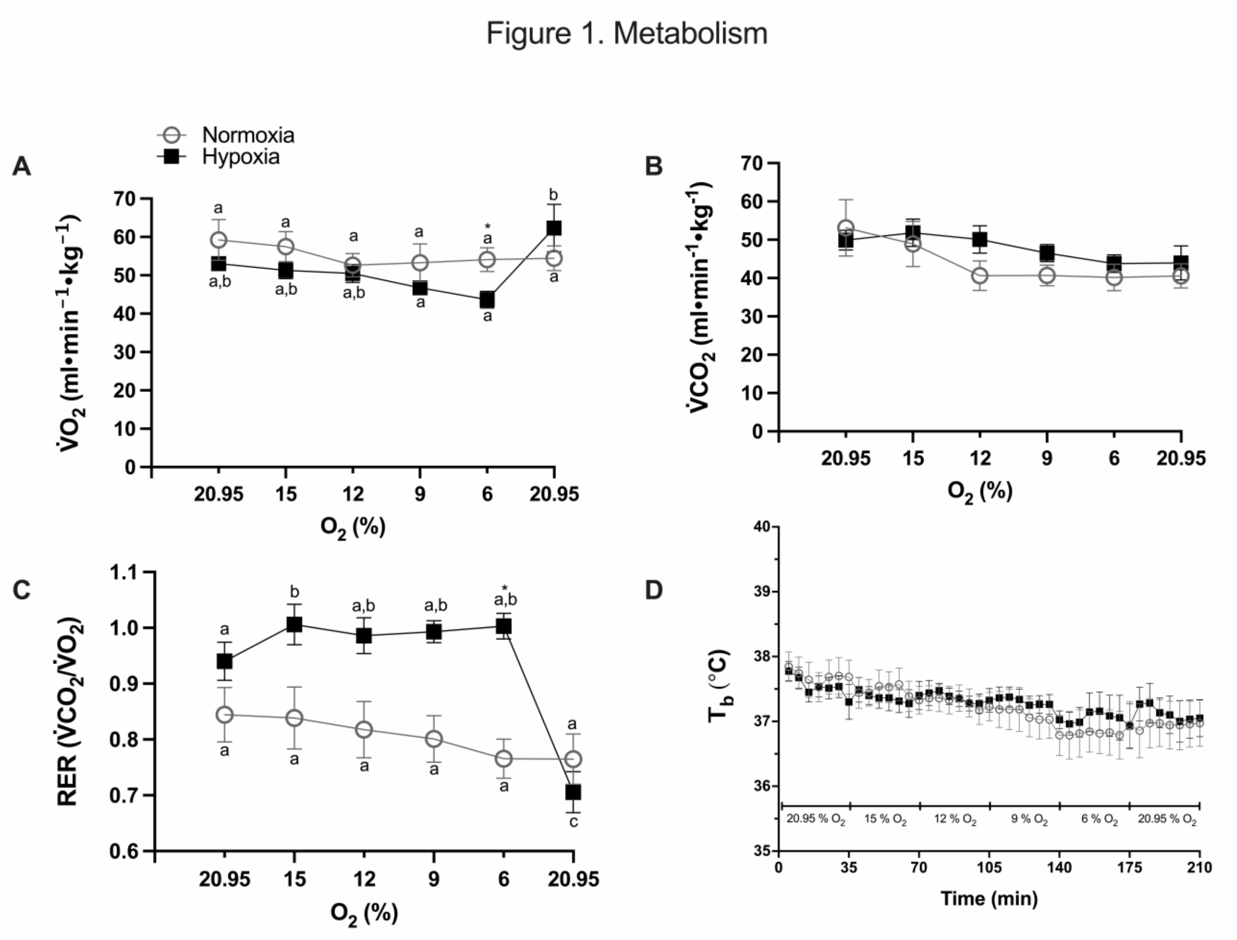

Figure 1. Metabolic and thermal responses of star-nosed moles exposed to acute hypoxia. A) Oxygen consumption rate ($\dot{V}O_2$), **B)** carbon dioxide production rate ($\dot{V}CO_2$), **C)** respiratory exchange ratio (RER), and **D)** body temperature (T_b) of star-nosed moles during 210 mins of either normoxia (open circles, n = 7), or 35-min exposures of step-wise decreasing hypoxia and a 35-min normoxic recovery period (squares, for O_2%=20.95-9, n=8; O_2%=6, n=7; O_2%=20.95/Recovery, n=6). Data were analyzed by REML with Sidak's and Tukey's multiple

comparisons tests ($p<0.05$, presented as mean ± S.E.M). Time course measurements that do not share the same letter are significantly different, whereas significantly different values between normoxia and hypoxia are denoted by asterisks.

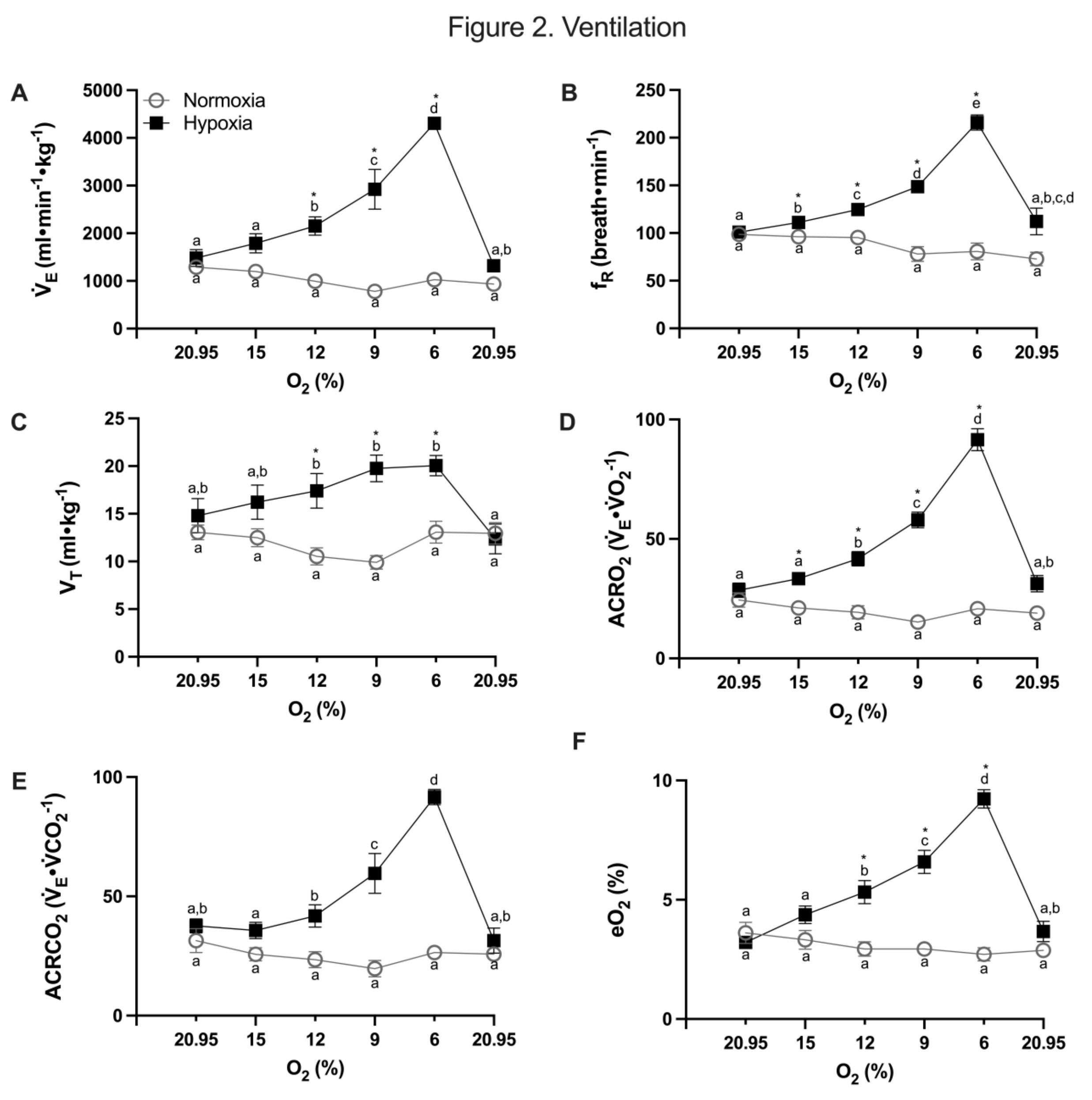

Figure 2. Ventilatory responses of star-nosed moles exposed to acute hypoxia. A) Minute ventilation ($\dot{V}_E$), **B)** respiratory frequency (f_R), **C)** tidal volume (V_T), **D)** air convection requirement of oxygen ($ACRO_2$), **E)** air convection requirement of carbon dioxide ($ACRCO_2$), and **F)** oxygen extraction efficiency (eO_2) of star-nosed moles during 210 mins of either normoxia (open circles, n = 7), or 35-min exposures of stepwise decreasing hypoxia and a 35-

min normoxic recovery period (squares, for O_2%=20.95-9, n=8; O_2%=6, n=7; O_2%=20.95/Recovery, n=6). Data were analyzed by REML with Sidak's and Tukey's multiple comparisons tests ($p<0.05$, presented as mean ± S.E.M). Time course measurements that do not share the same letter are significantly different, whereas significantly different values between normoxia and hypoxia are denoted by asterisks.

Table S1. Metabolic and ventilatory responses of juvenile vs. adult star-nosed moles to acute hypoxia. Mean ± S.E.M. and p-values of Sidak's multiple comparison test between adult and juvenile star-nosed moles, with sample sizes for each presented in parentheses.

Click here to download Table S1

Table S2. Metabolic and ventilatory comparisons of star-nosed moles during normoxia and hypoxia trials. Mean ± S.E.M. and p-values of Sidak's multiple comparison test between normoxic and hypoxic protocols for pooled adult and juvenile data, with sample sizes presented in parentheses.

Click here to download Table S2

Table S3. Metabolic and ventilatory timecourse comparisons of star-nosed moles during normoxia and hypoxia trials. Mean ± S.E.M. and p-values of Tukey's multiple comparison between time points within the normoxic and hypoxic protocols for pooled adult and juvenile data, with sample sizes presented in parentheses.

Click here to download Table S3